# RADIONUCLIDE CHARACTERIZATION OF A PLUTONIUM-CONTAMINATED SHEAR-BALER

Richard Thomason, Brian Young, and Ram Venkataraman,
Canberra Industries, Inc., Meriden, CT USA

Richard Ratner and Jason Watts
Nuclear Fuel Services, Erwin, TN USA

## ABSTRACT

Canberra has performed a radionuclide characterization of a shear-baler – a massive, durable machine used to shear equipment and glove boxes into suitable chunks and compact the chunks into bales of size 16 x 16 inches square and 4 to 10 inches thick. The compacted equipment items were removed from a shut down plutonium fuel fabrication facility. The shear-baler is being retired from service, and characterization data were needed to meet transportation and disposal requirements. The characterization was performed using both gamma-ray measurement and neutron counting techniques. The gamma-ray measurements were performed using the Canberra *In Situ* Object Counting System (ISOCS™). Because of the thick, reinforced steel walls of the shear-baler, gamma- ray measurements were not usable in some important regions of the shear-baler. Neutron measurements, with their higher transmission through the massive steel structure, were used to augment the gamma-ray measurements. Neutron counts were taken using a slab detector and JSR-12 electronics. Totals neutron count rate data were interpreted using a Monte Carlo – Neutron, Photon computer code (MCNP) model of the shear-baler. The neutron emission rate per gram of $^{239}$Pu was determined from samples of holdup material cleaned from the shear-baler. The neutron emission rate was expressed in terms of $^{239}$Pu for ease of comparison of the gamma-ray and neutron measurement results. The measurements were performed in several phases and were used to guide clean out of excess contamination from the shear-baler. The measurement program and analysis are described and results are reported.

Presented at
Show location
July 2003
Phoenix, AZ

# RADIONUCLIDE CHARACTERIZATION
# OF A PLUTONIUM-CONTAMINATED SHEAR-BALER

Richard Thomason, Brian Young, and Ram Venkataraman,
Canberra Industries, Inc., Meriden, CT USA

Richard Ratner and Jason Watts
Nuclear Fuel Services, Erwin, TN USA

## INTRODUCTION

As obsolete nuclear process facilities are decommissioned and deconstructed, the resulting contaminated equipment and building debris must be characterized for disposal. Some of the equipment items cannot be assayed using routine nondestructive techniques. A shear-baler at Nuclear Fuel Services (NFS) fits the difficult-to-assay category. It had been used to reduce the volume of plutonium-contaminated equipment from a decommissioned fuel fabrication facility. The task of the shear-baler at NFS was complete and the machine was to be disassembled into three sections for shipment to a disposal site. Shipping and disposal of the equipment sections required that the total, average surface, and average mass contamination of each section be determined to show that the shipment and disposal were in accordance with Federal and State regulations. This report describes the gamma-ray and neutron measurements performed to determine the $^{239}$Pu contamination on the shear-baler and presents the results of the measurements. Gamma-ray and neutron measurements were performed at NFS in the Spring of 2002, additional gamma-ray measurements were made in the Fall, and final gamma-ray and neutron measurements were completed in April 2003.

## SUMMARY

An experimental determination of the $^{239}$Pu remaining in a massive piece of discarded process equipment has been performed. Two largely independent methods were used and gave complementary and supportive results. The neutron method was calibrated based on samples of holdup removed from the shear-baler itself. This method was a powerful tool in assay of the shear-baler because neutrons are scattered but not heavily absorbed by the massive steel structure. The neutron measurement data were used in an optimization procedure in which the plutonium deposits in each of ten zones, chosen based on knowledge of the design and operation of the shear-baler, were determined. A Canberra ISOCS was used for the gamma-ray measurements. Because of the massive steel construction and reinforcement of the shear-baler, some parts were not suitable for gamma-ray assay. The evaluated results of the measurement campaign are:

17.4 g $^{239}$Pu in the shear ram assembly
including the compression head.

2.1 g $^{239}$Pu in the compression ram duct
and hydraulic cylinder.

0.8 g $^{239}$Pu in the hopper and greenhouse
assembly.

Activities for thirteen additional radioisotopes were obtained from the $^{239}$Pu activity by scaling based on data obtained from NFS. The radionuclide activities, activity sums, and activities per gram and per square cm for each of the three assemblies were tabulated. Those detailed data are not included in this report. Each major subassembly – shear ram assembly, compression ram duct, and hopper/greenhouse assembly – was shown to contain less than 100 nCi/g of transuranic activity and therefore was classified as low-level waste according to DOE Regulations.

## SHEAR-BALER DESCRIPTION

Pictures of the shear-baler while under construction are shown in Figure 1. Drawings of the shear-baler from the north and east sides are shown in Figures 2 and 3, respectively. The shear-baler consists of a hydraulic power unit, a feed hopper/charging chamber, a shear ram, and, at right angles to the shear ram, a compression ram. The shear head is 51.9 inches wide, 15.9 inches high, 52.5 inches long, and was driven by three 10 inch hydraulic cylinders providing

525 tons of force. The compression head is 15.9 inches square by 68 inches long and driven by a single 12 inch hydraulic cylinder providing 210 tons of force. In operation, the item to be compacted was lowered into the feed chamber, the shear ram was driven forward, shearing a 16 inch section from the lower part of the item and forcing the sheared material into a volume having the width and height of the shear head, and a depth of 16 inches. The shear head was left in place at the far limit of travel creating the second side wall of the compression chamber, and the compression ram was driven forward, compacting the material into a bale of dimensions 16 inches by 16 inches by 4 to 10 inches thick. The bale was ejected through the end gate into a glove box where it was deburred, wrapped, and bagged out. The shear and compression rams were then retracted for the next cycle.

To shear and compact the types of equipment items processed by the shear-baler, the machine had to be of extremely rugged design and construction. Most surfaces are a minimum of one inch steel plate. The shear head has a six inch thick front plate, a two inch rear plate, one inch plate on its sides and bottom, and three horizontal and three vertical internal stiffeners of one inch plate. The compression head is of similar construction to the shear head, but it has a two inch thick front face and one horizontal and one vertical one inch internal stiffener. Shear-baler walls along the shear ram length of travel are reinforced 2½ inch steel, compression chamber walls are 2½ inches thick, and the compression head guide channel walls are two inches thick. In the shutdown configuration, the shear ram is fully retracted and the compression ram is fully extended. The end gate is four inches thick and is in the closed (down) position.

## CONTAMINATION LOCATIONS

During the operating life of the shear-baler, it retained most of the radioactive contamination resulting from the shear and compaction processes. The outer surfaces of the shear-baler were expected to be relatively clean except for small quantities of contamination deposited during the disassembly process. Most internal contamination is in the L-shaped “duct/trough” in which the shear and compression rams traveled. The locations of contamination in this duct/trough are defined by sequential zones from the containment wall behind the shear head to the containment wall behind the compression head. Distance (**x**) along the shear ram trough is referenced to the east side of the end gate assembly; this is the easternmost surface of the shear-baler. Distance (**y**) along the compression ram duct is referenced to the north face of the end gate assembly. The surfaces used for reference are those that form the northeastern corner of the shear-baler. Height (**z**) is relative to the main floor level.

**Figure 1.**
The shear-baler while under construction showing, at left, the hydraulic power unit and shear ram cylinders and, at right in the foreground, the compression ram assembly connected to the heavily-reinforced compression chamber. The hopper, greenhouse, and operator’s station are shown in both pictures.

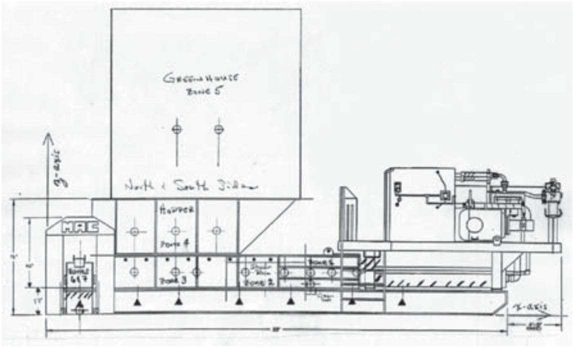

**Figure 2.**
Drawing showing features of the shear-baler from the north side. The heavy lines show boundaries of the various zones into which the baler was subdivided.

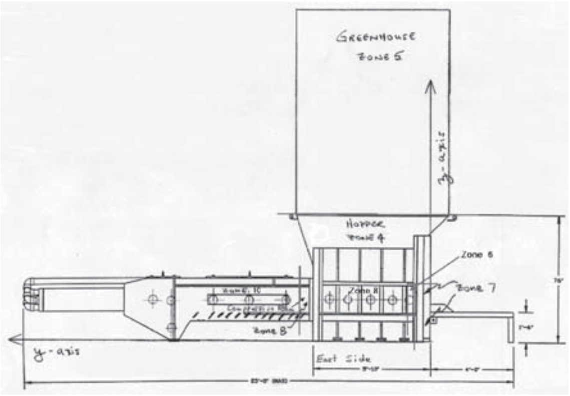

**Figure 3.**
Drawing showing features of the shear-baler from the east side. The heavy lines show boundaries of the various zones into which the baler was subdivided. The compression head is fully extended, as shown.

To organize the assays and analysis, the vicinity of the shear-baler was divided into ten zones:

Zone 1: Shear ram containment duct behind the fully retracted shear head. (x = 170 to x = 206 in.).

Zone 2: Current location of shear ram in the containment box/trough. (x = 118.5 to x = 170 in., fully retracted).

Zone 3: Charging chamber (x = 30 to x = 118.5 in.).

Zone 4: Hopper above charging chamber (Zone 3).

Zone 5: Greenhouse (containment box) above hopper (Zone 4).

Zone 6: Compression chamber (x = 14 to x = 30 in., y = 9 to y = 13 inches).

Zone 7: End gate and gate arm recess (x = 9.8 to x = 34.2 in., y = 4.8 to y = 9.0 in.).

Zone 8: Current location of compression ram (y = 13 to y = 81 in., fully extended).

Zone 9: Air intake and filter above secondary ram, removed after initial set of assays (y =108 to y =139 in.).

Zone 10: Compression ram containment duct behind compression head (y = 81 to y = 184 in.).

## ASSAY METHODS

### *Gamma-Ray*

The method using gamma-rays has the advantage of directionality, and so the location of significant deposits of contamination can generally be identified. However, the thick steel components and walls of the shear-baler significantly attenuated the gamma-rays. The gamma-ray measurements were performed using the Canberra ISOCS hardware and software. The ISOCS used a high-resolution gamma-ray detector that was heavily shielded and strongly collimated. The ISOCS software includes calibration templates for over twenty configurations of material. Six of these were used in the course of the analysis. The calibration and operation of the ISOCS was verified by assaying a known standard at NFS using a geometry definition appropriate to the standard. As part of measurement control, the standard was assayed prior to, at intervals through, and following each set of ISOCS measurements.

### *Neutron*

The neutron assay method provided an advantage over gamma assay of the shear-baler because the steel structure of the shear-baler does not attenuate neutrons to nearly the extent it attenuates gamma-rays. However, the quantification method using neutrons requires knowledge of $\eta$, the neutron emission rate per gram of $^{239}$Pu for the radioactive contamination in the shear-baler. The value of $\eta$ depends on the specific radioactive isotopes present, their relative fractions, and their physical form and chemical composition. The plutonium isotope and $^{241}$Am fractions of the shear-baler deposits were reasonably well known, but the physical and chemical forms were not. Material collected in recent clean outs of the shear-baler was used to determine $\eta_{actual}$ for held up material from the shear-baler. Only the totals counts (not coincidence counts) were used for the quantification calculations due to low coincidence neutron count rates. Calculation of the $^{239}$Pu mass from neutron count data for a simple case of one source and one detector is as follows:

$$M_{Pu} = R / \varepsilon / \eta_{actual}$$

where: $M_{Pu}$ = $^{239}$Pu mass in the deposit [g],

R = slab detector net count rate with the detector in a specific position [c/s],

$\varepsilon$ = efficiency for counting neutrons from the deposit with the detector at that position [c/n], and

$\eta_{actual}$ = neutron emission rate per gram of $^{239}$Pu in the deposit material [n/s/g].

The actual analysis used an optimization method to determine the $^{239}$Pu mass at each source location. The method will be summarized in the Neutron Measurements section below. Induced fission and spallation contributions to the neutron counts were assumed to be zero. Contributions from these sources are small or negligible for this application, and this assumption both simplifies the analysis and is conservative. Background count values were determined to be zero in the course of the optimization process.

## CALIBRATION

### *Gamma-Ray*

An ISOCS detector comes from the factory already characterized. It is calibrated for a specific assay configuration by defining the assay geometry using the ISOCS Geometry Composer. The detector characterization parameters are used by ISOCS routines to calculate a geometry-specific efficiency curve. An appropriate geometry model was used for each assay point. To verify that the ISOCS factory calibration was valid at the time of the shear-baler measurements, an NFS calibration standard was assayed using the ISOCS with a geometry definition appropriate for the standard. Assay results were in good agreement with the certificate value for the standard.

### *Neutron*

The neutron detector used in the shear-baler characterization was a block of polyethylene of about 3 x 7 x 43 inches containing five one meter long neutron detector tubes, each tube containing $^{3}$He at four atmospheres. The pulse-processing unit was a JSR-12 coincidence counter. Count data were read from the JSR-12 display and manually recorded. A $^{252}$Cf source was used to demonstrate that the performance of the counter did not change over the course of the measurements at NFS.

To calculate the mass of held-up $^{239}$Pu, the detector efficiency, $\varepsilon$, for counting neutrons from specific regions of the shear-baler for each detector position had to be determined. This efficiency was calculated from the geometry and composition of the structural material and the detector using the MCNP computer code. In this case, $\varepsilon$ is the probability that a neutron emitted by held-up material in a specific region (with specific geometry and containment) will be counted by the slab detector in a specific position relative to the deposit.

The neutron counting system was calibrated using samples of held-up material removed from the shear-baler. The geometry for the count of each sample was modeled using MCNP, and the counting efficiency for the sample, $\varepsilon_S$, determined. Using these data, the actual emission rate, $\eta_{actual}$, for each sample was calculated by the following equation, and results are shown in Table 1:

$$\eta_{actual} = R_S / \varepsilon_S / M_{Pu}$$

where: $M_{Pu}$ = $^{239}$Pu mass in the sample [g] determined by ISOCS (gamma assay), and

$R_S$ = Totals neutron count rate [c/s].

The value $\eta_{actual}$ in neutrons per second per gram of $^{239}$Pu is a calibration parameter for the neutron counting system. It, in fact, calibrates the neutron counting system for the form of material that is to be quantified in the shear-baler. Since NIST-traceable standards for the material in the shear-baler do not exist, $\eta_{actual}$ was not determined directly by a NIST-traceable standard. However, the ISOCS was originally calibrated and periodically checked using NIST-traceable standards, and the ISOCS was used to determine the $^{239}$Pu content of the shear-baler material samples. This method of calibration of the neutron counter for the shear-baler characterization is appropriate, and is the best feasible calibration that could be done for this particular application. The results from item five were not included in the weighted averages in Table 1 because that sample included a mixture of chips from two locations. The $\eta_{actual}$ values for the compression ram duct and the end gate were each determined by only a single sample, but given the relatively low statistical uncertainty of each of the resulting three emission rates relative to their differences, it was deemed appropriate to use the emission rate applicable to each zone for $^{239}$Pu mass determination.

## GAMMA-RAY MEASUREMENTS

For the initial sets of gamma assays, ISOCS assay live times were generally preset from 300 seconds to 1800 seconds. For the last set, live times of 1800 to 7200 seconds were used.

In the first set of ISOCS counts the air intake/filter was in the field of view of the detector at most assay locations, potentially causing the assay values to be inflated. Following the first set of counts, the intake/filter was removed and was absent for the other sets of measurements. Problems were encountered also during the second set of ISOCS assays inside the containment area. Attempts to assay the shear ram duct from the south side were unsuccessful because the cover over the chip clean-out port had been removed and the region in the vicinity of the charging gate had a complex geometry with openings to the shear-baler interior. As a result of these geometry complexities, no further effort was made to obtain

**Table 1.**
Data for determination of parameter $\eta_{actual}$ for neutron calculations. Statistical uncertainties are given at one standard deviation.

| Item No. | Container No. | Location from which collected | Gamma Assay (ISOCS) | | Net Neutron Count | | $\eta_{actual}$ | |
|---|---|---|---|---|---|---|---|---|
| | | | $^{239}$Pu (mg) | 1-σ (%) | Rate (c/s) | 1-σ (%) | ((n/s)/g $^{239}$Pu) | 1-σ (%)* |
| 1 | 3515293 | Primary Ram Duct | 160 | 25.9 | 1.3 | 10.3 | 1413 | 29.6 |
| 2 | 3515483 | Primary Ram Duct | 22 | 54.3 | 0.76 | 17.4 | 5054 | 57.9 |
| 3 | 234312 | Primary Ram Duct | 2.3 | 5% | 0.064 | 46.2 | 2097 | 47.5 |
| 4 | 234313 | Primary Ram Duct | 8.4 | 5% | 0.23 | 10.9 | 1983 | 15.6 |
| 5 | 234314 | Mixed, Pri & Sec | 1.4 | 6% | 0.075 | 39.8 | 4191** | 41.4 |
| 6 | 234316 | Secondary Ram | 9.2 | 5% | 0.34 | 6.7 | 2665 | 13.0 |
| 7 | 234317 | Under End Gate | 13.9 | 5% | 0.24 | 12.8 | 1234 | 17.0 |
| Weighted Neutron Emission Rates: | | | Primary Ram Duct | | Weighted Avg of Items 1 - 4 | | 1822 | 13.2 |
| | | | Secondary Ram | | Item 6 | | 2665 | 13.0 |
| | | | End Gate | | Item 7 | | 1234 | 17.0 |
| * Includes 10% uncertainty in $\varepsilon_S$. | | | ** Mixed locations and large uncertainty; not included in Final Results | | | | | |

assay data from the south side of the shear-baler. Another aspect of gamma-ray assay tends to inflate the results for a massive waste item like the shear-baler: when a specific feature is modeled – trough, ram head, steel plate – the calculation assigns all detected counts to the item modeled. In reality, gamma-rays counted by the detector include background gamma-rays from sources beside or beyond the item modeled. These background gamma-rays may experience much less attenuation than gamma-rays from the region being assayed, so they can cause a disproportionate increase in the assay value. Such background effects are difficult to identify and correct. This effect tends to cause assays of holdup deposits in the vicinity of other holdup (radionuclides) to be biased high. Finally, the assumed distribution of held-up material can affect assay results. For example, part of the input to some geometry templates is the relative activity concentration on each surface containing held-up material. In the case of the rectangular pipe template, for example, the relative concentration on each of the four interior and four exterior surfaces must be specified. The choice of these concentration values can strongly affect the results.

Given the potential and actual problems listed above, it is clear that, even after several carefully planned assay sessions, there were large uncertainties in some ISOCS assay values for the shear-baler. In fact, the massive steel content and location of the shear and compression heads makes determination of their holdup by gamma assay a practical impossibility. The ISOCS assay results by zone are shown in Table 2.

## NEUTRON MEASUREMENTS

Counts were made with the detector in twenty-six locations. The locations were chosen at roughly two foot intervals along each side of each ram duct. The twenty-six locations effectively surrounded the parts of the shear-baler that were expected to contain the major share of the contamination. The initial set of neutron counts was made in Spring 2002. The second and final set of counts was made in April 2003 with the detector in locations identical to those used in 2002.

Monte Carlo calculations modeling neutron transport in the shear-baler were performed using the MCNP code. Figure 4 shows a cross-section through the ram heads of the model developed for the shear-baler, and the detector locations on the east side of the shear-baler. Similar models were constructed for detector locations on the other three sides. The calculation for each of the four sets of detectors and one defined source term required one MCNP run. To obtain all needed efficiency data for the analysis required forty-four separate MCNP runs.

Interpretation of the detector count rates was done by modeling the principal features of the shear-baler and specifying the locations of likely depositions of contamination within the shear-baler containment. Seven areas of deposition, or source terms, were assigned to logical subdivisions of the assembly, such as the containment “box” behind the shear head, the shear head itself, the walls and floor of the charging chamber, and so on. Some of these source terms (the charging chamber, for example) were split into two

**Table 2.**
Gamma-ray assay results using ISOCS. The air intake and filter (Zone 9) were removed before these measurements were made.

| Zone | Description | $^{239}$Pu (g) | Uncert (%) | Comment |
|---|---|---|---|---|
| 1 | Duct Behind Shear Head | <6.4 | MDA | Minimum Detectable Activity (no peak) |
| 2 | Shear Ram Head | 121 | 25 | Too high: Filter source and low efficiency |
| 3 | Charging Chamber under Hopper | 2.8 | 30 | |
| 4 | Hopper (above Zone 3) | <0.3 | 35 | |
| 5 | Greenhouse (above Zone 4) | <0.5 | 46 | |
| 6 | Compression Chamber and End Gate | – | – | Spatial resolution insufficient to isolate |
| 7 | Under End Gate Arms | 1.8 | 17 | Value depends on verbal thickness info |
| 8 | Compression Ram | <214 | MDA | Too high: Filter source and low efficiency |
| 9 | Air Intake and Filter | – | – | No longer in vicinity of S-B |
| 10 | Duct Behind Compression Ram | 1.4 | 41 | |

separate source terms to test for asymmetry in the solution. This resulted in a total of ten source terms. MCNP calculations were made to determine the detector efficiency for counting neutrons from each source term at each detector position. The results of these calculations were then used to define a set of twenty-six equations, one for each detector location. Each equation summed the contributions from all source terms, with each source term multiplied by an unknown neutron emission rate, giving the calculated count rate for the corresponding detector location. An optimization was then performed to minimize the differences between the calculated and measured count rates at all detector locations, determining a "best" set of the ten source term rates. Dividing these source term rates by the appropriate values of $\eta_{actual}$ gave the $^{239}$Pu mass solution to the assay problem using the neutron approach. The paired source terms defined for the asymmetry tests were combined, resulting in the source term results given in this report. The calculated count rate fits to the final set of neutron count data are shown in Table 3.

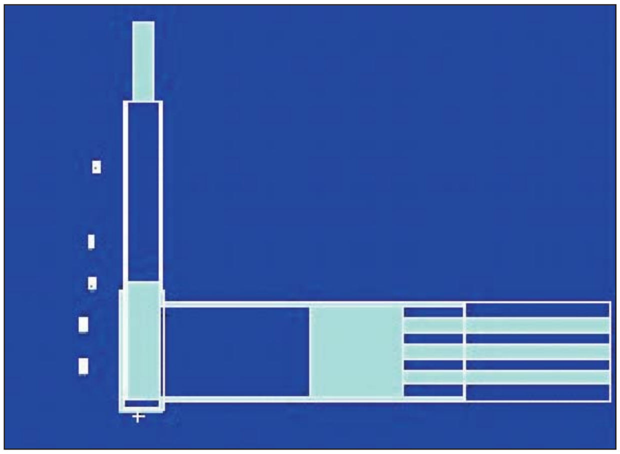

**Figure 4.**
Cross-section of shear-baler showing neutron detector positions on the east side.

The differences may be explained by variations in the concentration of deposit material that were not reflected in the relatively large, homogeneous source terms. The final reduced Chi Squared value (0.96) is very good considering the possible differences between the model distributions and actual deposits. In spite of these differences, the model masses should be a reasonably good representation of the relative mass distributions among the various source terms. The sum of the measured mass values should be an accurate measure of the total $^{239}$Pu mass in the vicinity of the shear-baler, with a lower relative uncertainty than that for the individual source terms.

**Table 3.**
Comparison of model and optimization results with the final set of measured count rates at each detector position.

| Detector Positions | Measured Rate | Measured Rate Unc | Model Rate | % Difference Model/Meas - 1 |
|---|---|---|---|---|
| N1 | 4.48 | 0.15 | 2.61 | -41.8 |
| N2 | 3.91 | 0.14 | 4.06 | 3.8 |
| N3 | 4.30 | 0.15 | 4.65 | 8.3 |
| N4 | 6.19 | 0.18 | 5.89 | -4.9 |
| N5 | 4.18 | 0.14 | 5.17 | 23.6 |
| N6 | 4.37 | 0.15 | 3.97 | -9.1 |
| N7 | 3.91 | 0.14 | 3.93 | 0.6 |
| N8 | 3.70 | 0.14 | 3.76 | 1.8 |
| N9 | 2.77 | 0.12 | 2.70 | -2.3 |
| E1 | 2.99 | 0.12 | 3.87 | 29.6 |
| E2 | 4.57 | 0.15 | 4.46 | -2.4 |
| E3 | 5.93 | 0.17 | 6.87 | 16.0 |
| E4 | 9.19 | 0.21 | 7.00 | -23.9 |
| E5 | 4.41 | 0.15 | 6.26 | 42.0 |
| S1 | 11.41 | 0.24 | 11.41 | 0.0 |
| S2 | 10.24 | 0.23 | 10.33 | 0.9 |
| S3 | 9.49 | 0.22 | 9.72 | 2.4 |
| S4 | 8.88 | 0.21 | 8.44 | -4.9 |
| S5 | 6.94 | 0.19 | 6.93 | -0.1 |
| S6 | 5.13 | 0.16 | 5.58 | 8.8 |
| S7 | 3.87 | 0.14 | 3.70 | -4.2 |
| S8 | 3.09 | 0.12 | 2.86 | -7.3 |
| W1 | 10.00 | 0.22 | 7.76 | -22.4 |
| W2 | 6.27 | 0.18 | 6.60 | 5.3 |
| W3 | 4.57 | 0.15 | 5.66 | 23.8 |
| W4 | 3.50 | 0.13 | 3.49 | -0.2 |
| Chi Squared = 15.40 | | | Source Terms = 10 | |
| Deg. of Freedom = 16 | | | Fitted Measurements = 26 | |

Results of analysis of the final set of neutron count rate data are shown in Table 4. Where no mass values are shown, that entry was either not included in the neutron transport model or was included in an adjacent zone for the analysis. The uncertainties are large because of the combination of uncertainties in the optimization process, the neutron model calculations, and in the value of $\eta_{actual}$.

**Table 4.**
Results of MCNP shear-baler model calculations and source term optimization. The air intake/filter (Zone 9) was removed before the final measurements were made.

| Zone | Description | $^{239}$Pu (g) | % TotUncert | OptimUnc (%) |
|---|---|---|---|---|
| 1 | Duct Behind Shear Head | 3.5 | 59 | 45 |
| 2 | Shear Ram Head | 4.4 | 53 | 36 |
| 3 | Charging Chamber under Hopper | 12.4 | 40 | 10 |
| 4 | Hopper (above Zone 3) | – | – | – |
| 5 | Greenhouse (above Zone 4) | – | – | – |
| 6 | Compression Chamber and End Gate | 0.4 | 107 | 100 |
| 7 | Under End Gate Arms | – | – | – |
| 8 | Compression Ram | 0.8 | 75 | 65 |
| 9 | Air Intake and Filter | – | – | – |
| 10 | Duct Behind Compression Ram | 2.7 | 43 | 20 |
|  | Other Uncertainty Contributions: |  | Model Shortcomings: | 25% |
|  |  |  | η Statistical Uncert: | 13 –17% |
|  |  |  | η Material Uncert: | 25% |

All uncertainties are 1 sigma. Contributions to the total relative uncertainty (*% TotUncert*) of the $^{239}$Pu quantities are as follows:

> Optimization Uncertainty (*OptimUnc %*): The value of each uncertainty contribution was estimated from the sensitivity of the associated mass to changes in the model.
>
> Model Shortcomings: This 25% contribution reflects errors in the model that result from differences between the model representation of the shear-baler and the details of the actual unit itself.
>
> η Statistical Uncertainty: The propagated uncertainty in this parameter is 13-17%. (Table 1.)
>
> η Material Uncertainty: 25% is an estimate of the uncertainty due to potential variations in the composition of deposit material at different locations in the shear-baler.

These contributions are all independent; thus the total uncertainty is obtained by adding the four contributions in quadrature.

## EVALUATED RESULTS AND UNCERTAINTIES

Table 5 summarizes the gamma and neutron assay results and in the last two columns presents the “best” assay and uncertainty results. The basis for selection of the “best” mass value and its uncertainty for each zone is given below. In making a selection of these best mass values, the very different nature of the gamma and neutron analyses were considered. Gamma-rays are heavily attenuated by a few inches of steel. Also, each gamma-ray analysis is independent of the others. For example, gamma-ray measurement of the holdup around the compression head may be impossible, but measurement of the holdup in the adjacent compression ram duct can be relatively accurate. On the other hand, neutron measurements are valid for massive steel structures as long as appropriate modeling calculations and calibration techniques are used. Unlike the independent gamma-ray assays, neutron analysis couples the solutions for all defined source terms. In this case, some source terms coming from the model may be higher or lower than actual, but the sum of all source terms should give an accurate value for the total $^{239}$Pu content of this system. That is, the sum of the mass solutions from the neutron model has higher credibility than the individual mass solutions themselves. The neutron analysis indicates 24 grams of $^{239}$Pu are in or around the shear-baler.

**Table 5.**
Summary of results: the "Best" mass values and 1-σ relative uncertainty are explained in the text.

| Zone | Description | Gamma | Neutron | "Best" Values | |
|---|---|---|---|---|---|
| | | (g $^{239}$Pu) | (g $^{239}$Pu) | g $^{239}$Pu | 1-σ % Uncert |
| 1 | Duct Behind Shear Head | <6.4 | 3.5 | 3.5 | 59 |
| 2 | Shear Ram Head | 121 | 4.4 | 4.4 | 53 |
| 3 | Charging Chamber under Hopper | 2.8 | 12.4 | 7.6 | 63 |
| 4 | Hopper (above Zone 3) | <0.3 | – | 0.3 | 35 |
| 5 | Greenhouse (above Zone 4) | <0.5 | – | 0.5 | 46 |
| 6 | Compression Chamber and End Gate | – | 0.4 | 1.1 | 24 |
| 7 | Under End Gate Arms | 1.8 | – | – | – |
| 8 | Compression Ram | <214 | 0.8 | 0.8 | 75 |
| 9 | Air Intake and Filter | – | – | – | – |
| 10 | Duct Behind Compression Ram | 1.4 | 2.7 | 2.1 | 31 |

The mass assignments were made as follows:

Zone 1: The neutron result is bounded by the gamma minimum detectable activity value. Use the neutron assay result of 3.5 g $^{239}$Pu and its 59% 1-σ uncertainty.

Zone 2: The gamma result is invalid. Use the neutron assay result of 11.4 g $^{239}$Pu and its 53% 1-σ uncertainty.

Zone 3: There are two "good" mass determinations for this zone, but the neutron result is four times the gamma-ray result. In Zone 10 the neutron result is two times higher. Since both gamma-ray and neutron results are defensible, the gamma and neutron results were averaged and the uncertainty was set at half the difference.

Zones 4 and 5: There is too little plutonium contamination to use neutron methods to quantify holdup in these zones. Use the gamma-ray upper bounds of 0.3 and 0.5 g $^{239}$Pu and their associated uncertainties.

Zones 6 and 7: The compression chamber and end gate are both small regions and are adjacent. Given the small quantities of plutonium involved, average the gamma-ray and neutron analysis results.

Zone 8: The gamma result is invalid. Use the neutron assay result of 0.8 g $^{239}$Pu and its 1-σ uncertainty of 75%.

Zone 9: The air intake/filter was removed and is not included in this report.

Zone 10: Like Zone 3, this zone is characterized by defensible gamma-ray and neutron results. As for Zone 3, the gamma and neutron results were averaged and the uncertainty was set to half the difference.

The sum of the neutron assay masses over all zones is 24.2 g $^{239}$Pu, and the sum of the "best" masses over all zones is 20.3 g $^{239}$Pu, so the set of best values approximately equals the sum solution of the neutron analysis.